Journal of Thermal Analysis and Calorimetry (2018) 134:1395–1404
https://doi.org/10.1007/s10973-018-7246-3

Systematic study of the role played by $ZnCl_2$ during the carbonization of a chemically activated carbon by TG–MS and DSC

S. Tazibet[1] · L. F. Velasco[2] · P. Lodewyckx[2] · D. Abou M'Hamed[3] · Y. Boucheffa[4]

Received: 29 September 2017 / Accepted: 4 April 2018 / Published online: 17 April 2018

Abstract
In this study, thermal and calorimetric techniques are used in order to get a better insight into the progress of the carbonization process of a lignocellulosic material for activated carbon preparation. Therefore, the pyrolysis process of the precursor (olive waste) alone and in the presence of the activating agent ($ZnCl_2$) at different temperatures is followed via thermogravimetry–mass spectroscopy analysis. The mass loss and the temperature programmed desorption profiles of the signals *m*/*e* = 16, 18, 28, 30, and 44 allow the determination of the role of the activating agent during the synthesis of the activated carbons at different temperatures. In order to follow the changes in energy during the pyrolysis process, differential scanning calorimetry is used. The obtained results are linked to the properties of the activated carbons obtained at the different temperatures and characterized in a previous paper. In this manner, it is possible not only to determine the thermal events taking place during the pyrolysis process but also to unravel their impact on the textural, structural, and surface properties of the final materials.

Keywords Pyrolysis · Activated carbon · Olive waste · $ZnCl_2$ · DSC · TG–MS

Introduction

The recurrent development of new applications for specific materials makes it necessary to continually optimize their preparation conditions. Many researches are made on activated carbon, which is one of the most important adsorbents used in the world due to its large range of applications and its low cost. In this regard, it has been demonstrated that a tailored design of nanoporous carbons is crucial not only in traditional applications, such as adsorption in liquid and gas phase [1–3], gas storage [4, 5], catalysis [6, 7], and electrochemistry [8, 9], but also in more recent uses as gas sensors, photocatalysts, and solar cell components [10, 11].

The use of activated carbons in such specific applications needs an excellent control of their porosity and surface functional groups. This is only possible by understanding the different phenomena occurring during the preparation of this material, especially during the activation and pyrolysis steps. However, these two operations depend on both the precursor and the activating agent used during the carbon elaboration. Specifically, and since Algeria is an important producer of olive oil, this study is focused in the valorization of olive stones by chemical activation with $ZnCl_2$. In fact, residual biomass is largely used for the production of activated carbon [12–17]. Nevertheless, the pyrolysis of these lignocellulosic materials is a chemically complex process in which several reactions occur simultaneously [18, 19].

With the aim of shedding light on this matter, we have carried out a systematic study of the progress of the carbonization process of this lignocellulosic material for the

✉ L. F. Velasco
leticia.fernandez@mil.be

[1] Ecole Militaire Polytechnique, 16111 Bordj El-Bahri, Algiers, Algeria

[2] Department of Chemistry, Royal Military Academy, Avenue de la Renaissance 30, 1000 Brussels, Belgium

[3] Laboratoire énergétique, Unité de Recherche-Développement Mécanique Aéronautique, 16100 Dar El-Beïda, Algiers, Algeria

[4] Laboratoire d'Etude Physico-Chimique des Matériaux et Application à l'Environnement, Université des Sciences et de la Technologie Houari Boumediene, B.P. 32, El-Alia, Bab-Ezzouar, Algiers, Algeria

preparation of activated carbon. Thus, in a previous work [20], four activated carbons were prepared at different temperatures by using olive waste as precursor and $ZnCl_2$ as activating agent. Since the surface chemistry of the activated carbon also plays an important role in its final applications, chemical activation was chosen in order to carefully study the formation of the surface groups. Then, the properties of the so-obtained materials were thoroughly characterized by means of N_2, CO_2, and H_2O adsorption, X-ray diffraction (XRD), Raman spectroscopy, Boehm titration, and Fourier transform infrared spectroscopy (FTIR). By studying the evolution of their properties with the carbonization temperature, we arrived to some interesting conclusions regarding the development of the porosity and the formation and location of the carboxylic groups, which are responsible for the moisture attraction during the adsorption process [21, 22].

In order to continue and complete the previous investigation, the pyrolysis treatment at various temperatures is herein in situ followed by means of thermogravimetric and calorimetric techniques. In this manner, the main products released during the pyrolysis of the precursor alone and in the presence of the activating agent are monitored by TG–MS analysis.

On the other hand, the changes in energy observed during the pyrolysis step of the mixture precursor/activating agent are measured by DSC. Moreover, and based on the pyrolysis phenomena evidenced by these techniques, the choice of the temperatures used to prepare the activated carbons is justified here.

The combination of all the obtained results leads to a better understanding of the role played by the activating agent during the carbonization step of a chemically activated carbon at different temperatures.

Experimental

Preparation of the samples

As it was mentioned before, olive stones (Bejaia region, Algeria) are used as a precursor for the preparation of the activated carbons. After cleaning, drying, and sieving the precursor, a chemical activation with $ZnCl_2$ (1:1 ratio) is carried out at four different temperatures (573, 653, 718, and 773 K). More details can be found in our earlier work [20].

Thermogravimetry–mass spectroscopy analysis (TG–MS)

The thermogravimetric analysis is performed using a TGA/SDTA 851 microbalance (Mettler Toledo) under argon flow (100 mL min^{-1}) with 25 mg of a mixture olive residue/$ZnCl_2$. The sample is heated from 298 K at 10 K min^{-1} until the desired temperature is reached (573, 653, 718, or 773 K), and then held constant for 1 h. These samples are named, respectively, AC573, AC653, AC718, and AC773 in reference to the operatory conditions for the preparation of the activated carbons studied in [20].

Additional measurements are carried out using 25 mg of the precursor (olive residue) alone in the same conditions. In this case, the so-obtained materials are named P573, P653, P718, and P773. By this approach, a comparative study of the results obtained for the precursor and for the mixture can be done in order to assess the impact of the activating agent in the carbonization process.

The TG apparatus is directly coupled to a Thermostar/Omnistar GSD 301 3T (PTM 62 113) mass spectrometer (Pfeiffer Vacuum). Gases are ionized by using a tungsten filament. The ion source parameters were optimized with argon. Hence, a correct setting of the cathode (40 V) prevents the formation of Ar^{++} ions and allows the detection of low H_2O concentrations on mass 18. Prior to each measurement, a blank is carried out by using an empty cell in the analysis conditions to ensure the stability of the signal and to evaluate the residual amount of each compound in the argon flow. MS signals m/e = 16, m/e = 18, m/e = 28, m/e = 30, and m/e = 44 are determined.

DSC analysis

DSC measurements of the precursor/activating agent mixture are carried out under the same operating conditions as the TG–MS measurements (previous section). However, and in order to avoid the presorbed water peak, each sample is held at 393 K for 20 min and then heated up to the final desired temperature.

A quantity of 30 mg is carbonized under a nitrogen flow (20 mL min^{-1}) in aluminum crucibles using Netzsch DSC 204 equipment, which is previously calibrated with indium and zinc.

All the TG–MS and DSC experiments are done in triplicate.

Results and discussion

TG–MS results

TG results

The pyrolysis at different temperatures of both the mixture olive residue/$ZnCl_2$ and the precursor alone is followed by TG measurements. The TG and DTG (first-derivative

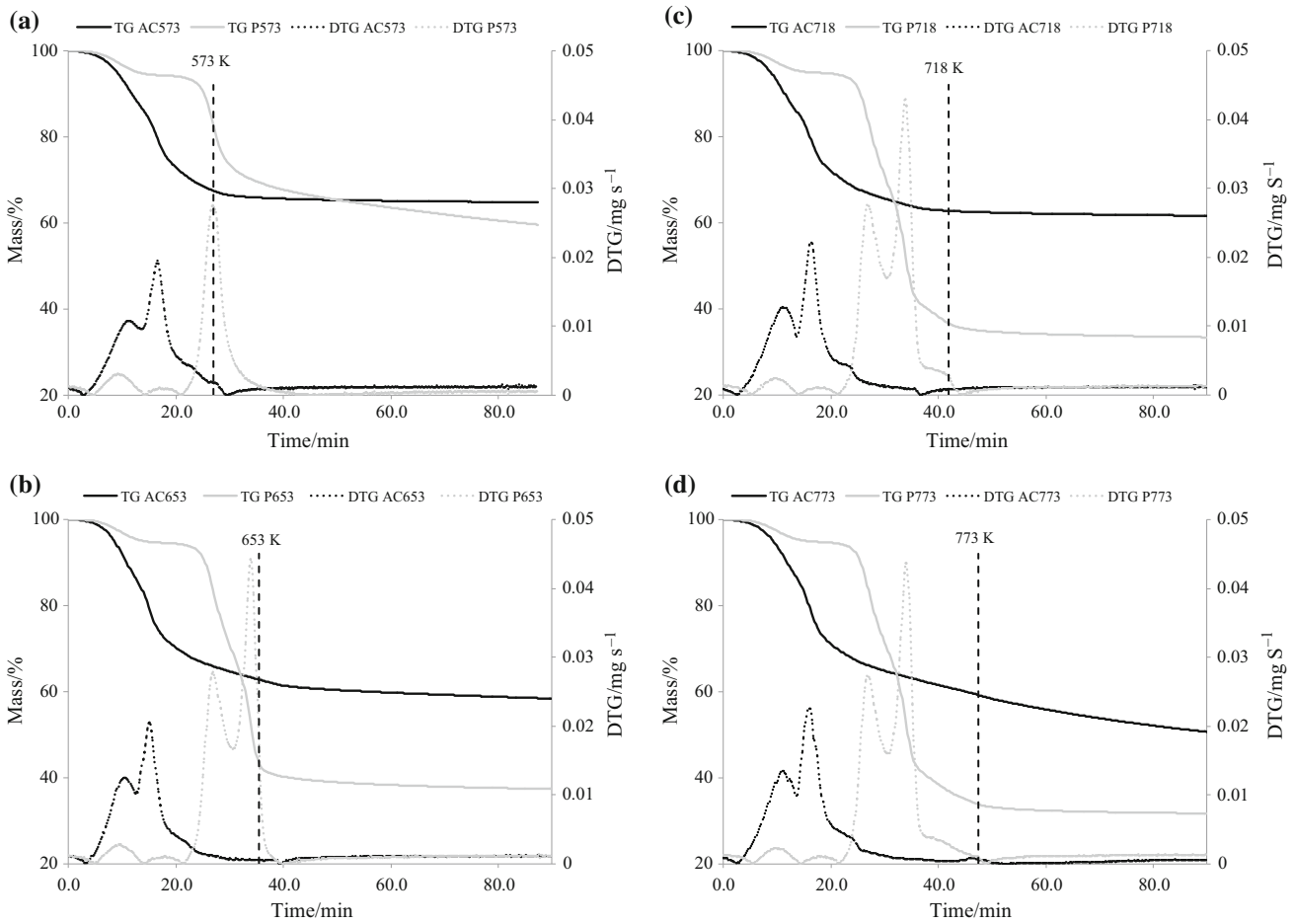

Fig. 1 TG and DTG curves of the precursor and the mixture during the pyrolysis at different temperatures: **a** 573 K, **b** 653 K, **c** 718 K, and **d** 773 K

thermogravimetric) profiles are given in Fig. 1a–d and Table 1.

The first observation is that all the curves present a mass loss at around 393 K, which corresponds to the first peak in the different DTG curves. This indicates the presence of physisorbed water in the precursor. In fact, and as it is discussed in [20], the precursor contains many oxygen groups susceptible to make hydrogen bonds with water molecules.

After the loss of presorbed water, the TG curves start to differ between the mixture and the precursor. Indeed, the mass loss of the precursor occurs at higher temperatures in two steps: the first one at about 573 K ($\sim$ 22%) and the second one at about 633 K ($\sim$ 35%) (Table 1). The first DTG peak at around 573 K is probably due to the hemicellulose and cellulose decomposition, as reported in the literature [23]. The thermal decomposition of lignin, which takes place in three steps, also contributes to this peak and is responsible for the one observed at 633 K and the small peak (shoulder) at around 718 K [24]. The fact that the yield of a char from cellulose carbonization at temperatures around 773 K is very low [23] indicates that sample P773 is mainly the result of hemicellulose and lignin transformations.

Since the peaks observed in the DTG profiles correspond to different thermal events, carbonization temperatures were specifically selected in order to separately study them.

In the presence of $ZnCl_2$, the mass loss is shifted to lower temperatures, and the DTG peak appears at 453 K (also with a shoulder), and no other peak is detected, except the one corresponding to water desorption (at 393 K). Consequently, the main mass losses occur at temperatures below 573 K (see Table 1). This phenomenon is already cited in the literature [25], stating that $ZnCl_2$ acts as a catalyst in all pathways of cellulose degradation: dehydration, depolymerization, and ring opening leading to a lightly oxygenated product and CO and CO_2 formation. Based on our results, this finding can also be extended to the thermal decomposition of lignin.

Total mass loss values are 35.2, 38.4, and 41.8% for AC573, AC653, and AC718 samples, respectively. In the

Table 1 Mass loss (%) of the precursor and the mixture at the selected pyrolysis temperature ranges

Temperature/K	P573	P653	P718	P773
298–573	21.2	23.0	22.8	22.5
573–573	19.2			
573–653		34.3	35.2	35.1
653–653		5.4		
653–718			5.5	5.9
718–718			3.2	
718–773				2.7
773–773				2.3
Total	40.4	62.7	66.7	68.4
Temperature/K	AC573	AC653	AC718	AC773
298–573	32.9	33.7	33.7	34.5
573–573	2.3			
573–653		2.7	2.8	2.7
653–653		2.1		
653–718			1.8	2.0
718–718			3.5	
718–773				1.6
773–773				10.6
Total	35.2	38.4	41.8	51.4

case of AC773, this value goes up to 51.4%, which is the result of a noticeable mass loss (10.6%) during the isothermal step at 773 K.

The total mass loss of the precursor alone is much higher than for the mixture, especially for the samples pyrolyzed at temperatures of 653, 718, and 773 K. Therefore, the presence of $ZnCl_2$ positively altered and accelerated the pyrolysis and increased the carbon yield [26].

Water TPD profiles

Given that the precursor used (olive residue) is a lignocellulosic material containing hydrolysable functional groups such as hydroxyls [26], the loss of water is of great importance during the degradation of this material. Therefore, the m/e = 18 TPD profiles are explored (Fig. 2).

The first observation is that the water TPD profiles can be superposed perfectly with the DTG curves (Fig. 1a–d), for both the precursor and the mixture. This means that the mass loss during the pyrolysis process is mainly due to the departure of water molecules.

Secondly, it is observed that the precursor and the mixture exhibit different TPD profiles, indicating a different behavior during the pyrolysis process.

In the case of the precursor, all the obtained TPD profiles contain three peaks, except for the sample P573 which, logically, does not present the third peak at around 633 K. The first peak in the water TPD profiles of the precursor is obtained at around 393 K, and it is assigned to the desorption of presorbed water. In fact, lignocellulosic materials contain adsorbed moisture due to their polar nature [27]. In this regard, the water isotherm presented in [20] shows the relatively big amount of interactions between water molecules and the surface of the precursor. On the other hand, the two peaks obtained at higher temperatures correspond to the loss of water from chemical reactions [27].

The mixture precursor/$ZnCl_2$ curves present one water peak at around 453 K for all the samples. However, the DTG curves show two peaks in this region, so we suppose that the water peak is the combination of the presorbed water at around 393 K and the water coming from the dehydration of the precursor. The temperature of this phenomenon is lower than that of the precursor alone due to the presence of $ZnCl_2$, which plays a role as a catalyst.

TPD profiles of other compounds

Some other degradation compounds formed during the pyrolysis of both the precursor and the mixture were followed by MS. The different TPD profiles are given in Fig. 3a–d.

At this point, it is important to clarify that the overall purpose of the MS analysis was to qualitatively compare the TPD profiles of the mixture and the precursor in order to evaluate the influence of the activating agent ($ZnCl_2$) on the pyrolysis process, and not to carry out an exhaustive determination of all the species formed. Accordingly, MS signals corresponding to m/e = 16, 28, 30, and 44 were selected in order to monitor the main species produced during the thermal degradation of lignocellulosic materials and which mainly consist of carbon dioxide (CO_2), carbon monoxide (CO), light hydrocarbons (primarily CH_4), and small amounts of other gases [23, 28].

The release of some volatile compounds, in terms of their m/e ratio, during the pyrolysis at different temperatures is resumed in Table 2.

First of all, it is observed that the intensities of the TPD profiles of these compounds (Fig. 3) are lower than those of water (Fig. 2) [22].

As expected, and based on the DTG results, in the case of the mixture precursor/$ZnCl_2$ all the compounds appeared at lower temperatures in comparison with the precursor alone. This phenomenon is partially found in the literature, where Khelfa et al. [25] studied the effects of some inorganic salts like $ZnCl_2$ on cellulose pyrolysis. Related to this, and in order to understand the lignocellulosic pyrolysis, many researchers investigated the degradation of cellulose, hemicellulose, and lignin separately [23, 25, 29–31] or by combining two compounds (cellulose–hemicellulose [31, 32], cellulose–lignin

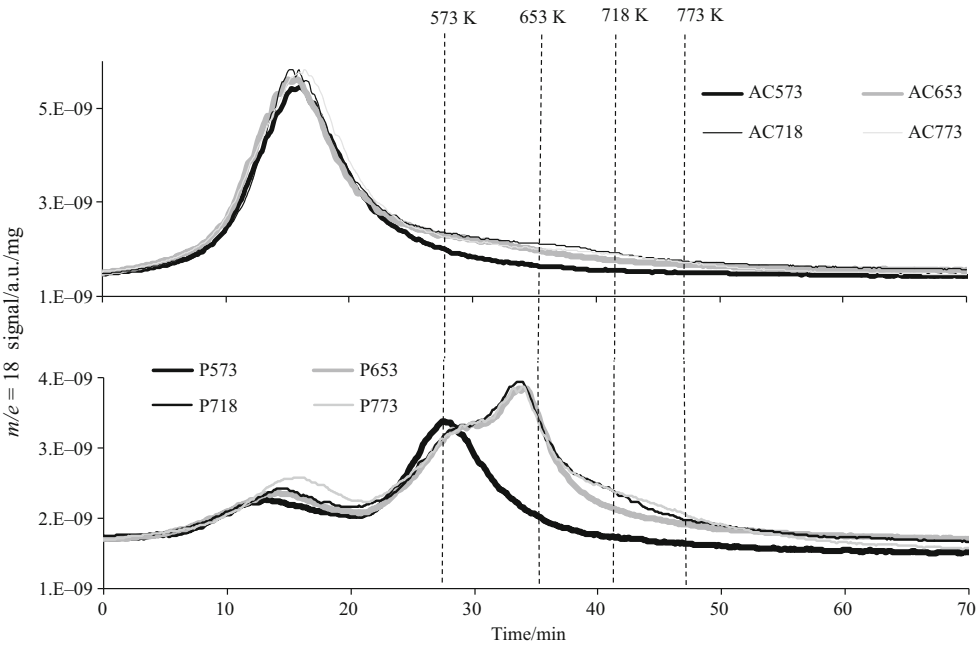

Fig. 2 *m/e* = 18 TPD profiles obtained by mass spectrometry during the carbonization of the precursor and the mixture during the pyrolysis at different temperatures

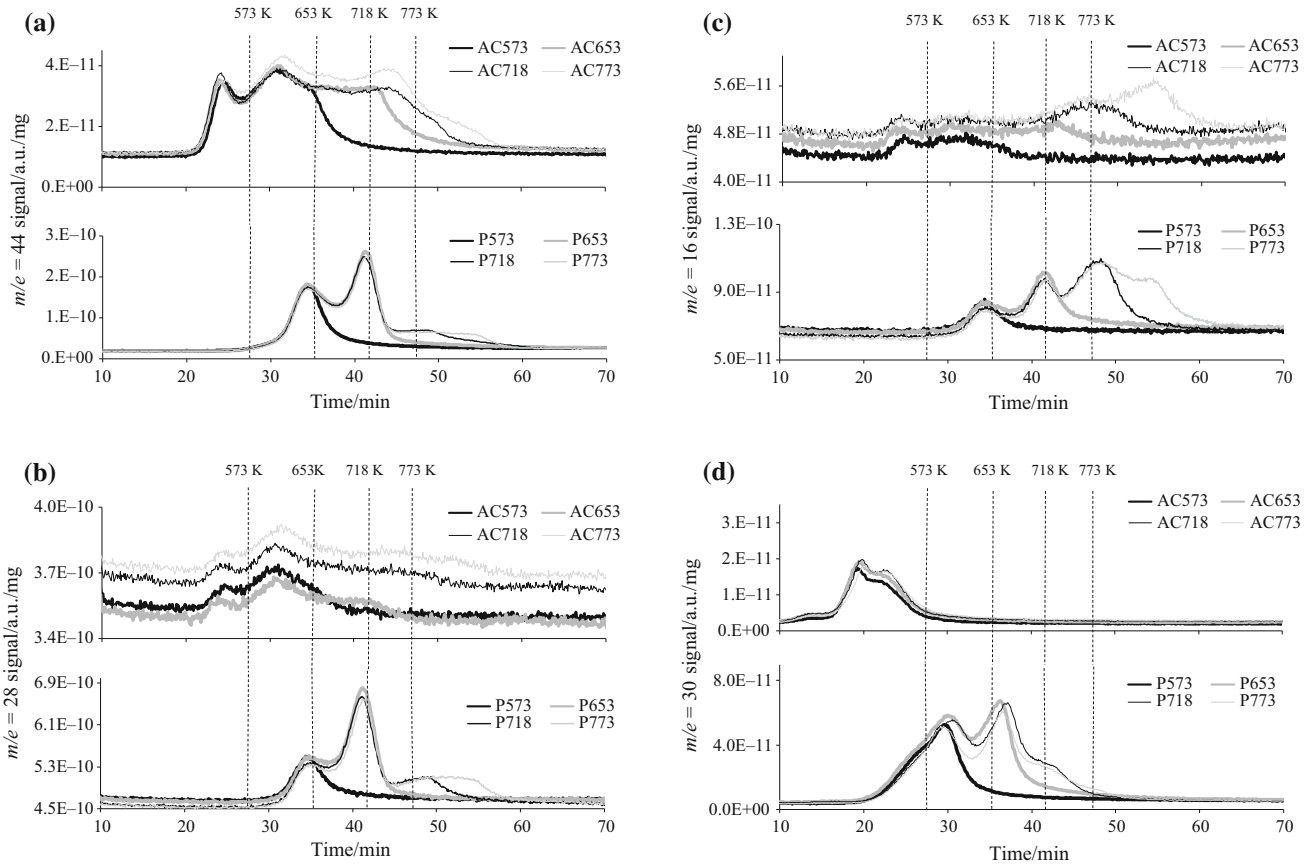

Fig. 3 TPD profiles obtained by mass spectrometry during the carbonization of the precursor and the mixture at different temperatures: **a** *m/e* = 44, **b** *m/e* = 28, **c** *m/e* = 16, and **d** *m/e* = 30

Table 2 Evidence of some volatile compounds released during the pyrolysis of both the mixture and the precursor

	< 573 K	573–653 K	653–718 K	718–773 K	773 K
Mixture precursor/$ZnCl_2$					
m/e = 44	+	+	+	+	+
m/e = 28	+	+	+	+	+
m/e = 16	+	+	+	+	+
m/e = 30	+	−	−	−	−
m/e = 18	+	−	−	−	−
Precursor					
m/e = 44	−	+	+	±	±
m/e = 28	−	+	+	+	+
m/e = 16	−	+	+	+	+
m/e = 30	+	+	+	+	−
m/e = 18	+	+	+	+	−

− no peak, ± small peak, + intense peak

[31, 33]). The study of the combination of the three compounds has also been done [31, 34]. However, it is still difficult to attribute, with certitude, the provenance of the different compounds, due to their interactions during the pyrolysis step, especially between cellulose and lignin [31–33].

Bearing in mind that a given *m/e* ratio can correspond to different compounds with the same molecular weight, it is probable that both formaldehyde (CH_2O) and to a lesser extent, ethane (C_2H_6) are contributing to the *m/e* = 30 signal. Specifically, formaldehyde is formed during the dehydration of cellulose [23], and probably also hemicellulose, while ethane is formed at higher temperatures during the thermal decomposition of lignin [24, 35]. This is consistent with the results shown in Figs. 2 and 3, where *m/e* 30 is the only signal detected during the dehydration of the materials. This phenomenon is observed in both the precursor and the mixture. However, and as mentioned before, due to the role of the $ZnCl_2$ as a catalyst, the thermal processes take place at lower temperature for the mixture than for the precursor alone.

The *m/e* = 28 and 44 TPD profiles of the precursor, which can be mainly ascribed (as explained below) to the formation of CO and CO_2, respectively, are very similar in terms of peak shape and intensity. However, this trend is not seen in the mixture, especially above 653 K. Indeed, the pyrolysis of olive residue in the presence of zinc chloride leads to more CO_2 than CO. This is probably due to the departure of carboxylic acid groups which are formed below a temperature of 573 K. The amount of these functions decreases seriously for the samples AC718 and AC773 [20]. Furthermore, the decomposition of carboxylic groups yields mainly CO_2 [36, 37]. Also, and in agreement with the fact that $ZnCl_2$ accelerates the pyrolysis process, CO_2 is detected at lower temperatures for the mixture than for the precursor alone. Previous results on cellulose decomposition show much higher production of CO and CO_2 over other gaseous products [23]. Given that olive stones are lignocellulosic materials and that low pyrolysis temperatures ($T \leq 773$ K) were used, we consider that CO_2 and CO are mainly produced, and that is the reason why we assign the signals *m/e* = 44 and *m/e* = 28 mainly to these two compounds. Nonetheless, one has to note that the formation of acetaldehyde, which has been reported for the thermal decomposition of cellulose [23], and propane can also slightly contribute to the *m/e* = 44 signal, whereas ethylene can have a small influence on the *m/e* = 28 signal.

Finally, the signal *m/e* = 16, which can be principally attributed to CH_4, is investigated (Fig. 3c). In the case of the precursor, the departure of CH_4 seems to be linked with *m/e* signals 28 and 44. The production of CH_4 is mainly due to the lignin decomposition; therefore, the CH_4 peaks in the profiles of Fig. 3c appeared at higher temperatures. It is an indication that CH_4 evolves from the pyrolysis of lignin between 573 and 733 K. The release of this species at higher temperature can be ascribed to the secondary degradation of primary unstable volatile species [34]. However, CH_4 TPD profiles of the mixture seem different from those of *m/e* 28 and 44, which can probably point to other mechanisms. In fact, the differences between the TG–MS profiles of the precursor and the mixture are probably due to the role of $ZnCl_2$ as a catalyst. In this sense, dehydration at lower temperatures (mixture precursor/$ZnCl_2$) lowers the amount of hydrogen and oxygen atoms from the lignocellulosic precursor earlier and thus lessens the chance of polymerization [26].

Following pyrolysis by DSC

The DSC curves of the olive waste/precursor mixture are given in Fig. 4. The results show two exothermic peaks common for all samples, the first at 453 K and the second

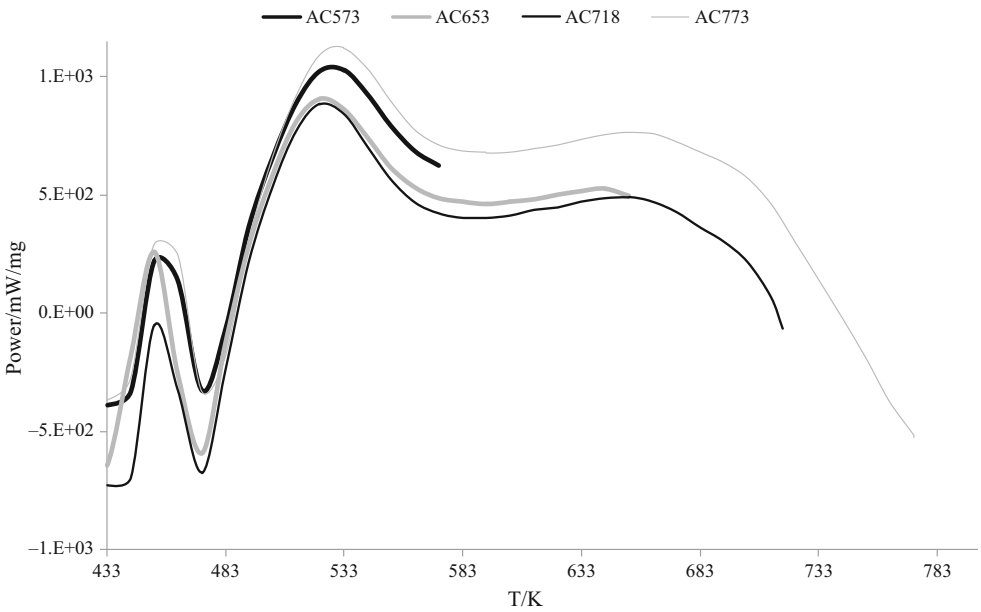

Fig. 4 DSC curve of the activated carbon samples during the carbonization

one at 523 K. A third large peak appears at higher temperature, with a maximum at 653 K. The first peak can be assigned to the dehydration process; in fact, a similar peak detected at this same temperature is observed in the water TPD profiles. The second peak is also an exothermic one; it seems to correspond to phenomena involving volatiles such as CO_2 and CO (Fig. 3). It is important to note that, despite the fact that the dehydration process leads to a considerable mass loss, the energy produced during the dehydration is small if compared to that produced later. In addition, dehydration seems to be an independent phenomenon, characterized by a well-resolved peak, contrary to the phenomena happening at temperatures higher than 473 K. The third peak is the largest with a maximum around 653 K and does not overlap any TPD profiles mentioned in the previous section. So we can suggest that this peak is a combination of many peaks provided from the different phenomena happening in the temperature range of 573–773 K, including the depolymerization process.

It has to be mentioned that during the isothermal step, a change in the signal is only detected for the sample AC773, where a considerable energy is measured (Fig. 5). In addition, during this step, this sample loses 10.6% of its mass, much higher than the mass loss measured during the isothermal steps at lower temperatures (Table 1). These two phenomena cannot be associated with CO, CH_4, and CO_2 release, because they are also observed during the isothermal step of the other samples (Fig. 3) and are probably due to the condensation of the carbon into graphite-like rings [24].

Relationship between pyrolysis process, porosity, structural properties, and surface functional groups of the activated carbons

During the preparation of activated carbons, the main chemical processes take place in the pyrolysis stage, where the maximum loss of mass and the biggest changes in structural, textural, and physicochemical properties occur [20].

The pyrolysis of lignocellulosic materials is a very complex process, and up to now, no mechanism has been proposed to adequately describe it. In this study, the aim is to try to link the pyrolysis phenomenon with the porosity and the functional groups of the resulting materials. Hence, the textural, structural, and surface properties of the materials presented in a previous study [20] can be now further discussed in terms of the herein-studied reactions taking place during the pyrolysis treatment.

Table 3 shows the BET-equivalent surface area of the samples pyrolyzed at the different temperatures. If we consider that the maximum of porosity is achieved at 718 K (S_{BET} = 1659 m^2/g), we can deduce that the pyrolysis at a temperature of 573 K (S_{BET} = 1035 m^2/g) leads to the creation of more than half ($\sim$ 60%) of the porosity. Thus, the dehydration process of the precursor in the presence of the catalyst $ZnCl_2$, leading to a change in the structure of the precursor as shown by X-ray diffraction (XRD) [20], is a crucial step in the development of the porosity of the activated carbon.

On the other hand, depolymerization, which occurs at higher temperatures (573 and 653 K) and releases some gaseous fraction containing CO, CO_2, and a heavy oil fraction with other volatile materials [26], is responsible for a further creation of

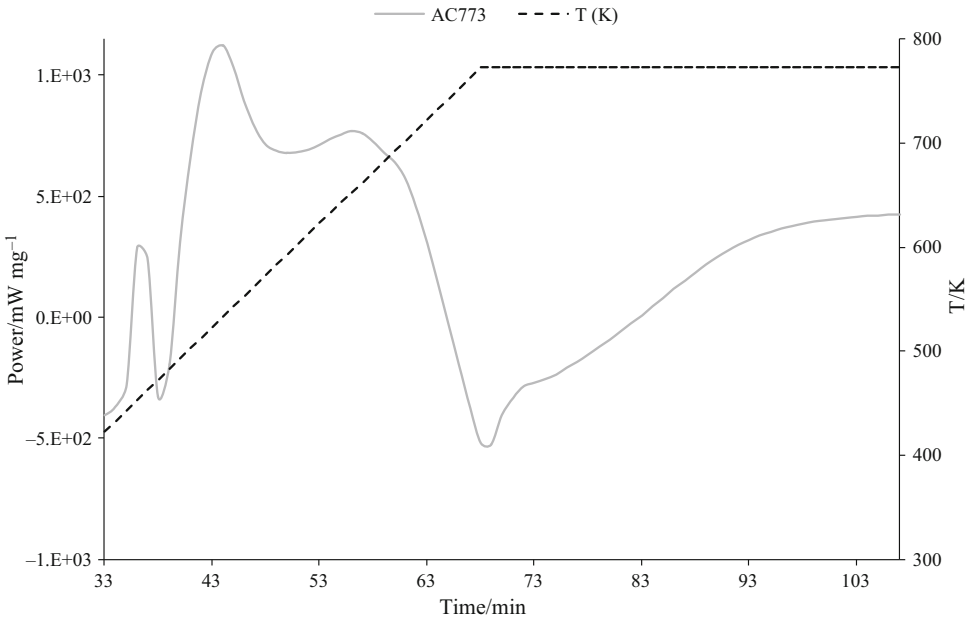

Fig. 5 DSC profile of the sample AC773, including the isothermal step at 773 K

Table 3 BET-equivalent surface area of the samples

Samples	AC573	AC653	AC718	AC773
$S_{BET}/m^2\ g^{-1}$	1035	1628	1659	1492
Temperature range/K	298–573	573–653	653–718	718–773
$\Delta S_{BET}/m^2\ g^{-1}$	+ 1029	+ 593	+ 31	− 167

porosity. In this way, and taking into account the similar S_{BET} values obtained for samples AC653 and AC718, we can conclude that the porosity is created during the dehydration and depolymerization processes, highlighting the role of the catalyst $ZnCl_2$ therein. In fact, this reactant is also behaving as a templating agent for the creation of porosity [17]. Moreover, carbonization at higher temperatures (773 K) has a negative effect on the textural properties of the obtained material due to the condensation of the carbon network. So we can suggest that at a temperature of 653 K, the performance of $ZnCl_2$ as a catalyst (on this precursor) is nearly optimal.

According to Boehm's titration results [20], the activated carbon prepared at a temperature of 573 K contains a high amount of carboxylic surface groups. These are created during the condensation of the species derived from the dehydration of cellulose and hemicellulose [34]. So the dehydration process leads to the creation of carboxylic groups. Some of these functions disappear during the depolymerization process up to a temperature of 653 K. The results show a decrease in the amount of carboxylic groups for the samples AC718 and AC773 due to the effect of the relatively high temperature. In this regard, we found in an earlier work that a temperature of 773 K is sufficient to eliminate carboxylic acidic groups from the surface of activated carbons [38]. However, the water isotherms [20] show very similar slopes for AC653 and AC773; this can be explained by the creation of carboxylic anhydrides at the temperature of 773 K, probably due to rearrangement reactions.

The *m/e* = 18 and 30 TPD profiles are similar, indicating that the departure of water and formaldehyde seems to be linked.

Boehm's titration permits a global quantification of the bases on the surface of activated carbons, but it cannot provide information about the nature of these bases. The results show that the bases depend on the pyrolysis temperature [20]. In fact, some bases disappear at 718 K, probably due to the lignin decomposition; in fact, we suspect that these bases are those of the lignin. However, another amount of bases is created when the pyrolysis is done at 773 K, so we suggest that these functions need a higher energy of formation and are stronger than the first ones. The departure of CH_4, which is provided from the lignin decomposition, can be related to this phenomenon.

It seems that the functional groups further influence the evolution of the porous structure. In fact, a significant amount of porosity (more than a third of the total) is created during the depolymerization process without significant mass loss (less than 3%—see Table 1); simultaneously, changes are noted concerning the surface functional groups composition, especially the decrease in the carboxylic groups. In addition, it is shown that the external functionalities of the cellulose affect the surface properties of the resulting activated carbons; these pendant groups create carbonaceous intermediates with different sizes and chemical properties [39].

Conclusions

In this work, the evolution of the carbonization process of a lignocellulosic material for activated carbon preparation and the role played by the activating agent have been further addressed by means of thermal and calorimetric analysis. The results gathered in this part of the work and the previous one [20] allow to determine the thermal events involved, but also contribute to a better understanding of their influence on the final properties of the carbon material. Thus, and based on the results obtained in both parts of the study, we can conclude that:

- The presence of $ZnCl_2$ positively alters and accelerates the pyrolysis and increases the carbon yield.
- The carboxylic surface groups of activated carbons prepared from a lignocellulosic precursor are created below a temperature of 573 K, due to the cellulose and hemicellulose dehydration.
- The dehydration process occurs at temperatures below 473 K and leads to a considerable mass loss. However, the energy produced during this step is small when compared with that produced at higher temperatures.
- The dehydration of the precursor in the presence of the catalyst $ZnCl_2$ is the most crucial step in the development of the porosity of the activated carbon. Thus, highly porous materials can already be obtained by carbonization at 573 K.
- The depolymerization process also contributes to the textural development of the material. Therefore, the performance of $ZnCl_2$ as a catalyst is nearly optimal at 653 K.
- The functional groups further affect the evolution of the porous structures.

References

1. Zhong L, Zhang Y, Ji Y, Norris P, Pan W-P. Synthesis of activated carbon from coal pitch for mercury removal in coal-fired power plants. J Therm Anal Calorim. 2016;123(1):851–60.
2. Yu F, Li Y, Han S, Ma J. Adsorptive removal of antibiotics from aqueous solution using carbon materials. Chemosphere. 2016;153:365–85.
3. Lodewyckx P. Adsorption of volatile organic vapours. In: Rufford TE, Zhu J, Hulicova-Jurcakova D, editors. Green carbon materials—advances and applications. Boca Raton: CRC Press; 2014. p. 235–56. ISBN 9789814411134.
4. Sethia G, Sayari A. Activated carbon with optimum pore size distribution for hydrogen storage. Carbon. 2016;99:289–94.
5. Melouki R, Llewellyn PL, Tazibet S, Boucheffa Y. Hydrogen adsorption on activated carbons prepared from olive waste: effect of activation conditions on uptakes and adsorption energies. J Porous Mater. 2017;24(1):1–11.
6. Sebastián D, Alegre C, Calvillo L, Pérez M, Moliner R, Lázaro MJ. Carbon supports for the catalytic dehydrogenation of liquid organic hydrides as hydrogen storage and delivery system. Int J Hydrogen Energy. 2014;39:4109–15.
7. Lam E, Luong JHT. Carbon materials as catalyst supports and catalysts in the transformation of biomass to fuels and chemicals. ACS Catal. 2014;4(10):3393–410.
8. Li Q, Zhu Y, Zhao P, Yuan C, Chen M, Wang C. Commercial activated carbon as a novel precursor of the amorphous carbon for high-performance sodium-ion batteries anode. Carbon. 2018;129:85–94.
9. Piwek J, Platek A, Krzysztof F, Frackowiak E. Carbon-based electrochemical capacitors with acetate aqueous electrolytes. Electrochim Acta. 2016;215:179–86.
10. Bandosz TJ. Nanoporous carbons: looking beyond their perception as adsorbents, catalyst supports and supercapacitors. Chem Rec. 2016;16:205–2018.
11. Gomis-Berenguer A, Velasco LF, Velo-Gala I, Ania CO. Photochemistry based on nanoporous carbons: perspectives in energy conversion and environmental remediation. J Colloid Interface Sci. 2017;490:879–901.
12. Kumar A, Jena HM. High surface area microporous activated carbons prepared from Fox nut (*Euryale ferox*) shell by zinc chloride activation. Appl Surf Sci. 2015;356:753–61.
13. Özdemir M, Bolgaz T, Saka C, Sahin Ö. Preparation and characterization of activated carbon from cotton stalks in a two-stage process. J Anal Appl Pyrolysis. 2011;92:171–5.
14. David E, Kopac J. Activated carbons derived from residual biomass pyrolysis and their CO_2 adsorption capacity. J Anal Appl Pyrolysis. 2014;110:322–32.
15. Correia LB, Fiuza RA Jr, de Andrade RC, Andrade HMC. CO_2 capture on activated carbons derived from mango fruit (*Mangifera indica* L.) seed shells: a TG study. J Therm Anal Calorim. 2018;131(1):579–86.
16. Gao F, Qu J, Zhao Z, Wang Z, Qiu J. Nitrogen-doped activated carbon derived from prawn shells for high-performance supercapacitors. Electrochim Acta. 2016;190:1134–41.
17. Marsh H, Rodriguez-Reinoso F. Activated carbon. Amsterdam: Elsevier Science & Technology Books; 2006.
18. Poletto M, Zattera AJ, Santana RMC. Thermal decomposition of wood: kinetics and degradation mechanisms. Bioresour Technol. 2012;126:7–12.
19. Yusof N, Ismail AF. Post spinning and pyrolysis processes of polyacrylonitrile (PAN)-based carbon fiber and activated carbon fiber: a review. J Anal Appl Pyrolysis. 2012;93:1–13.
20. Tazibet S, Velasco LF, Lodewyckx P, Abou M'Hamed D, Boucheffa Y. Study of the carbonization temperature for a chemically activated carbon: influence on the textural and structural characteristics and surface functionalities. J Porous Mater. 2017. https://doi.org/10.1007/s10934-017-0444-8.
21. Fletcher AJ, Uygur Y, Thomas KM. Role of surface functional groups in the adsorption kinetics of water vapor on microporous activated carbons. J Phys Chem C. 2007;111:8349–59.
22. Salame II, Bandosz TJ. Study of water adsorption on activated carbons with different degrees of surface oxidation. J Colloid Interface Sci. 1999;210:367–74.
23. Shen DK, Gu S. The mechanism for thermal decomposition of cellulose and its main products. Bioresour Technol. 2009;100:6496–504.
24. Nassarl MM, MacKay GDM. Mechanism of thermal decomposition of lignin. Wood Fiber Sci. 1984;16(3):441–53.
25. Khelfa A, Finqueneisel G, Auber M, Weber JV. Influence of some minerals on the cellulose thermal degradation mechanisms: thermogravimetry and pyrolysis-mass spectrometry studies. J Therm Anal Calorim. 2008;92:795–9.

26. Wu Q, Pan N, Deng K, Pan D. Thermogravimetry–mass spectrometry on the pyrolysis process of Lyocell fibers with and without catalyst. Carbohyd Polym. 2008;72:222–8.
27. Scheirs J, Camino G, Tumiatti W. Overview of water evolution during the thermal degradation of cellulose. Eur Polym J. 2001;37:933–42.
28. Kan T, Strezov V, Evans TJ. Lignocellulosic biomass pyrolysis: a review of product properties and effects of pyrolysis parameters. Renew Sust Energy Rev. 2016;57:1126–40.
29. Asmadi M, Kawamoto H, Saka S. Gas- and solid/liquid-phase reactions during pyrolysis of softwood and hardwood lignins. J Anal Appl Pyrolysis. 2011;92:417–25.
30. Shen DK, Gu S. Cellulose chemistry and technology. Cell Chem Technol. 2010;44(1–3):79–87.
31. Zhou H, Wu C, Meng A, Zhang Y, Williams PT. Effect of interactions of biomass constituents on polycyclic aromatic hydrocarbons (PAH) formation during fast pyrolysis. J Anal Appl Pyrolysis. 2014;110:264–9.
32. Shen D, Xiao R, Gu S, Zhang H. The overview of thermal decomposition of cellulose in lignocellulosic biomass. In: van de Van T, Kadla J, editors. Cellulose biomass conversion. Rijeka: InTech; 2013.
33. Wu S, Shen D, Hu J, Zhang H, Xiao R. Intensive interaction region during co-pyrolysis of lignin and cellulose: experimental observation and kinetic assessment. BioResources. 2014;9:2259–73.
34. Giudicianni P, Cardone G, Ragucci R. Cellulose, hemicellulose and lignin slow steam pyrolysis: thermal decomposition of biomass components mixtures. J Anal Appl Pyrolysis. 2013;100:213–22.
35. Calvo-Flores FG, Dobado JA, Isac-García J, Martín-Martínez FJ. Chemical characterization and modification of lignins. In: Materials Calvo-Flores FG, Dobado JA, Isac-García J, Martín-Martínez FJ, editors. Lignin and lignans as renewable raw. New York: Wiley; 2015. p. 189–246.
36. Thommes M, Morlay C, Ahmad R, Joly JP. Assessing surface chemistry and pore structure of active carbons by a combination of physisorption (H_2O, Ar, N_2, CO_2), XPS and TPD-MS. Adsorption. 2011;17:653–61.
37. Shen W, Li Z, Liu Y. Surface chemical functional groups modification of porous carbon. Recent Patents Chem Eng. 2008;1:27–40.
38. Tazibet S, Boucheffa Y, Lodewyckx P. Heat treatment effect on the textural, hydrophobic and adsorptive properties of activated carbons obtained from olive waste. Microporous Mesoporous Mater. 2013;170:293–8.
39. Sun M, Hong L. Impacts of the pendant functional groups of cellulose precursor on the generation of pore structures of activated carbons. Carbon. 2011;49:2173–80.